Physics Letters A 547 (2025) 130511

Contents lists available at ScienceDirect

Physics Letters A

journal homepage: www.elsevier.com/locate/pla

Letter

Deceleration of polar molecules by synchronous stimulated radiation force with low power light

Jin Wei [a], Di Wu [a], Taojing Dong [a], Chenyu Zu [a], Tao Yang [a,b], Yong Xia [a,b,c,*], Jianping Yin [a]

[a] State key laboratory of precision spectroscopy, School of Physics and Electronic Science, East China Normal University, Shanghai 200241, China
[b] Collaborative Innovation Center of Extreme Optics, Shanxi University, Taiyuan, Shanxi 030006, China
[c] NYU-ECNU Institute of Physics at NYU Shanghai, Shanghai 200062, China

ARTICLE INFO

Edited by Dr Suming Weng.

Keywords:
Molecule slowing
Stimulated force
Cold molecule

ABSTRACT

We propose a theoretical approach for rapid deceleration over short distance on polar molecules by using stimulated force combined with a phase compensation and frequency chirping. First, we simulate the dynamic processes of the decelerated magnesium fluoride (MgF) and ytterbium fluoride (YbF) molecules using the 3D Monte-Carlo method, and find that a buffer-gas-cooled molecular beam with a longitudinal velocity of 200 m/s can be decelerated to be below 5 m/s at a laser power of only 0.44 W for MgF and 0.21 W for YbF per traveling wave. Second, we estimate the number of molecules loaded into the magneto-optical trap (MOT). This scheme overcomes the spatial inhomogeneity of stimulated radiation force and reduces the high laser power requirement, which have not been reported before. Such new results will provide a timely useful way for optical slowing and loading the dense molecule species into a MOT for realization of quantum degeneracy.

1. Introduction

Compared to atoms, molecules have rich degrees of freedom - rotational and vibrational states - that can offer a new and fascinating platform for the study of encoding and processing quantum information [1,2], ultracold chemistry [3], precision tests of fundamental physics [4] and correlated quantum systems [5]. However, their complex level structure makes molecules more difficult to control reliably. Therefore, achieving ultracold temperatures and high densities for molecules is a crucial and challenging task. Following the rapid progress in direct laser-cooling techniques, chilling a dense collection of molecules into the quantum regime is already on the way. For example, magneto-optical trapping (MOT) of diatomic and polyatomic molecules have been realized on SrF [6], CaF [7,8], YO [9], BaF [10], and CaOH [11]. Furthermore, the 3D blue-detuned molasses has been reported to enable CaF and SrF to cool further down to 50 μK [8,12,13], which is well below the Doppler limit. Additionally, the loading of molecules into optical dipole traps [12], magnetic traps [13,14], and optical tweezer arrays [15] have been achieved. About 1.0×10^5 molecules, as a maximum number so far, has been captured by L. Anderegg et al. through a radio frequency CaF MOT [7]. Recently, the blue-detuned MOT for YO molecules have provided a phase-space density exceeding 10^{-6} in optical traps with a temperature of 8.8 μK [16]. In short, the application of these techniques to collisions and evaporative cooling may open a path toward quantum degeneracy, such as molecular Bose-Einstein condensation [5].

In general, for molecules to be captured by a MOT, they need to be slowed down below the capture velocity, which is typically below 20 m/s [17]. Laser radiation pressure slowing is a common method. So far, the number of molecules being captured in a MOT are limited by the relatively long distance, with losses caused by high vibrational dark states and transverse divergence in the deceleration process. Experimentally, deceleration of SrF was demonstrated with a frequency broadened slowing method [18]. Also, the frequency scanning techniques for radiation pressure beam slowing, was successfully applied to a few types of molecules, such as CaF [19,20], YO [21], CaOH [10], and BaF [11]. In contrast, some theoretical schemes for molecule deceleration and trapping have been proposed [22-24].

Different from the laser radiation pressure slowing above, many experimental proposals and theoretical calculations have been presented on using a bichormatic light force for molecular beam slowing with no experimental implementation [25–32]. Stimulated forces rely on the coherent control of momentum exchange through rapid absorption-stimulated emission cycles, producing a large net force with

* Corresponding author at: State key laboratory of precision spectroscopy, School of Physics and Electronic Science, East China Normal University, Shanghai 200241, China.
E-mail address: yxia@phy.ecnu.edu.cn (Y. Xia).

https://doi.org/10.1016/j.physleta.2025.130511
Received 14 December 2024; Received in revised form 22 March 2025; Accepted 31 March 2025
Available online 7 April 2025

appropriate laser power and sequencing. For a two-level system, the magnitude of this force can reach $\hbar k\delta/\pi$ with an optimal relative phase of $\pi/2$, which is larger than the maximum radiation pressure force of $\hbar k\gamma/2$ for $\delta > \gamma$ (δ is the detuning, γ is the natural line width and the wavevector $k = \frac{2\pi}{\lambda}$, λ is the wavelength, and $\hbar = h/2\pi$ (h is Planck's constant)) [33]. The velocity capture range of stimulated forces ($\delta/2k$) is also more favourable than that of radiative forces [34,35]. In 2011, Eyler et al. first studied the performance of the bichromatic forces on molecules with complex structures and internal degeneracies. Through numerical simulations, they found that a precooled CaF beam with a forward velocity of 130 m/s could be nearly brought to the capture speed of magneto-optical traps at a laser irradiance level of each travelling wave of 125.6 W/cm^2 [33]. In 2017, similar work was conducted on MgF deceleration to verify the effectiveness in molecular beam deceleration using stimulated force. A MgF beam with a forward velocity of 120 m/s can be decelerated to nearly several m/s using a laser irradiance per travelling wave of 127 W/cm^2 at a laser power of 0.99 W [36]. In 2018, our group theoretically investigated the possibility of slowing the heavy-atom molecules by coherent optical stimulated force with a constant beat phase. It shows that a YbF beam with a forward velocity of 120 m/s can be decelerated to below 10 m/s using a laser irradiance for each traveling wave at 107.2 W/cm^2 [37]. Particularly, in 2018, the deflection experiment was conducted on buffer-gas CaF and SrOH beams using the bichromatic force, which suggests the feasibility of applying stimulated force to decelerate molecular beams [26,27].

However, all the work above requires a high laser power to slow the molecular beam from 150 m/s to be within the MOT capture velocity range. Typically, the tightly focused laser beams with a top-hat diameter of 1 mm are used, necessitating continuous wave laser powers exceeding 1 W per traveling wave. The two-colour standing wave field contains four travelling wave fields, so the total laser power is at least 4 W. Using a larger detuning δ, at the cost of laser power requirements that scale with δ^2, it produces a faster note period and thus a larger force. The magnitude of the velocity-dependent force decreases significantly as the beat phase difference increases, which occurs when the molecular beam travels a short distance of several centimetres. A constant beat phase method is used to compensate the variation of this phase difference to maintain a large stimulated force while the molecules are being decelerated [38]. Nevertheless, since the stimulated force is only sizable for $|v| < \delta/2k$, and typically, the initial distribution of the molecules before deceleration tends to spread out, the deceleration forces are not uniformly applied to the molecular beam throughout the deceleration process. Consequently, during a force period, a substantial portion of molecules experience minimal force, more than half of the duration. This results in relatively lower average forces during deceleration, leading to a very low deceleration efficiency in a conventional stimulated deceleration scheme [38]. Thus, the efficiency of the interaction is reduced between the two-colour standing-wave laser field and the molecules.

Herein, to overcome both the high laser power requirements and the stimulated force inhomogeneous distribution on molecules, in this paper we theoretically demonstrate the longitudinal slowing of polar molecules using optical stimulated force combined with phase compensation and electro-optic modulator (EOM)-based frequency chirping. We choose MgF and YbF molecules to represent the light and heavy systems, respectively. The paper is organized as follows. Section 2 details our scheme and simulation approach. Section 3 presents the deceleration of cryogenic buffer-gas beams of MgF and YbF to the velocities suitable for MOT using a low laser power. Section 4 summarizes our results.

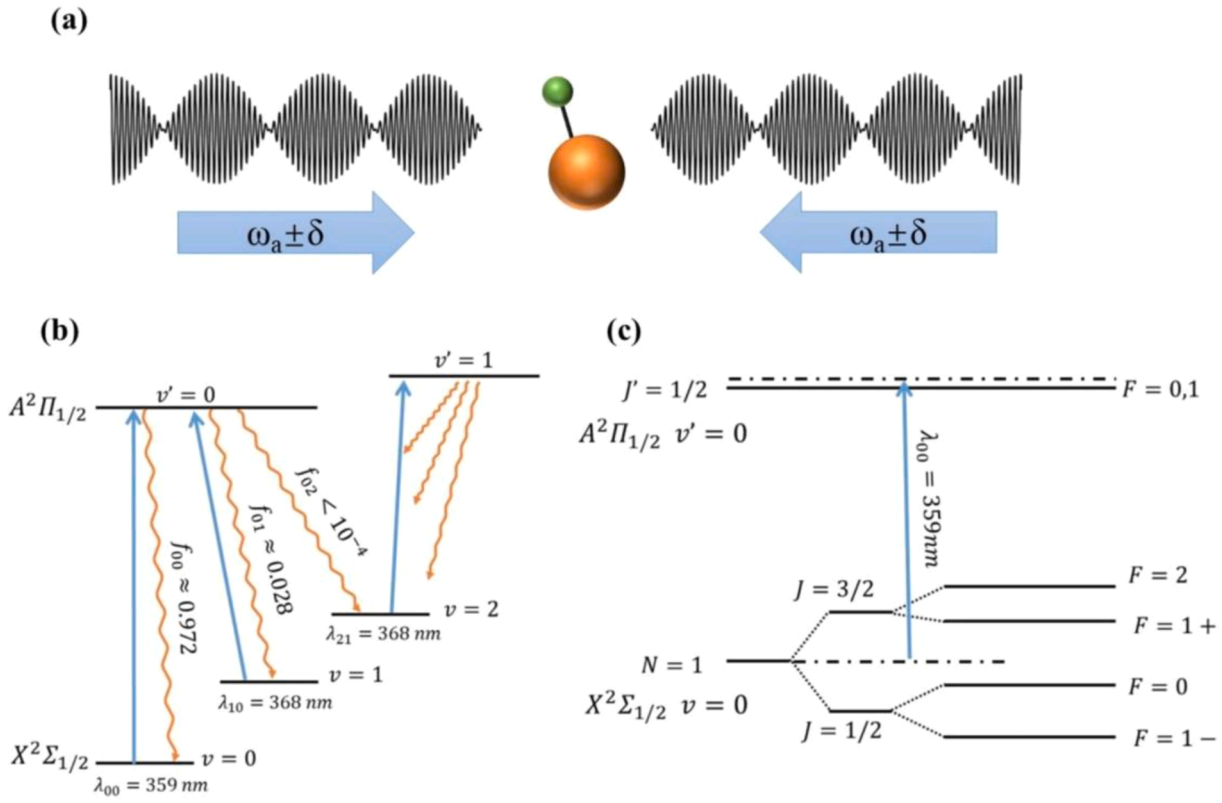

Fig. 1. (a) Sketch of the stimulated force on MgF molecule in a π-pulse model. The two laser beams travel in opposite directions, symmetrically detuned by δ from a carrier frequency ω_a. (b) The relevant vibrational levels and branching ratios of the $X \rightarrow A$ transition in MgF. (c) The energy structure of the main cooling cycle transition ($X^2\Sigma_{1/2}$ ($v = 0, N = 1$)$\rightarrow A^2\Pi_{1/2}$ ($v' = 0, J' = 1/2$)). The spontaneous emission from $A^2\Pi_{1/2}$ to $X^2\Sigma_{1/2}$ is controlled by the vibrational branching ratio $f_{v'v}$ (the downward orange curve in the Fig. 1(b)). Upward solid blue lines denote the transitions driven by lasers $\lambda_{vv'}$.

2. Deceleration scheme

2.1. Level structure of MgF

Fig. 1(a) shows the sketch of the stimulated force on a diatomic molecule in a π-pulse model [33]. The laser beams are symmetrically detuned by δ from a frequency ω_a. The vibrational energy structure of MgF and corresponding branching ratios between them are illustrated in Fig. 1(b). The structure of the $X^2\Sigma_{1/2}$ $(v=0, N=1) \rightarrow A^2\Pi_{1/2}$ $(v'=0, J'=1/2)$ branch is depicted in Fig. 1(c). The main cooling transition has $\lambda_{00} = 359$ nm, and the Franck-Condon factor f_{00} for this transition is 0.972 [39]. λ_{00} is the main slowing light with a natural linewidth of $\gamma = 2\pi \times 22$ MHz. With the repumping light λ_{10} and λ_{21}, the population accumulating in the vibrational states is repumped back. For the ground state $X^2\Sigma^+_{1/2}$, both the spin-rotation and hyperfine interactions split the $|X, N=1\rangle$ state into four components, which are characterized by the hyperfine quantum number $F = 2, 1+, 0, 1-$, and the energy intervals are 9 MHz, 120 MHz and 110 MHz, respectively. With the molecular constants for MgF listed in [40], we have:

$$\begin{aligned} |F=1^+, M\rangle &= 0.6990|(J=3/2)F=1, M\rangle + 0.7151|(J=1/2)F=1, M\rangle \\ |F=1^-, M\rangle &= -0.7151|(J=3/2)F=1, M\rangle + 0.6990|(J=1/2)F=1, M\rangle. \end{aligned} \tag{1}$$

M represents the magnetic quantum number and J represents the total angular momentum quantum number. Eq. (1) is used to calculate the electric-dipole matrix elements and hyperfine branching ratios for MgF.

2.2. Scheme of stimulated force deceleration

Here, we propose a scheme for the longitudinal slowing of polar molecules. This is achieved by using optical stimulated force combined with phase compensation and frequency chirping techniques. This ensures that the maximum force is synchronously applied to the molecules during the deceleration process, while eliminating the need for high-power lasers. We refer to this approach as synchronous stimulated force deceleration of molecules.

Fig. 2 shows the proposed design for producing the Doppler-shifted dual-colour field, compensating the phase difference changes, making the frequency chirped, and producing a molecular beam from a buffer-gas source. In short, the gas-phase MgF is produced by the laser ablation and entrained from a cryogenic buffer-gas cell [41]. The MgF molecules then enter the deceleration region after traversing a free flight region, and are subsequently probed. The incident light has a detuning of $-\delta$ from the ω_a and part of this light is shifted with an acoustic optical modulator (AOM) to $\omega_a + \delta$ and recombined with the unshifted beam $(\omega_a - \delta)$. The resulting beams are combined using a polarizing beam splitter (PBS) and then split by a beam splitter (BS). To maintain the deceleration of the molecules with the maximum force and to compensate for the Doppler shifts, we modulate the frequency through EOM_1 and EOM_2 (As shown in the green dashed box on the top side). The chirp rate can be precisely controlled. If the counter-propagating beat notes are properly sequenced, a large force will be generated by the alternation of cycles of coherent excitation and stimulated emission. The phase change could be adjusted by synchronizing the position of the optical delay line with the motion of molecules using stepper motors (As shown in the green dashed box on the bottom side).

The two counter-propagating travelling-wave lights are π-polarized with the chirped frequency of $\omega_a \pm \delta \pm kv(t)$, driving the transition of $X^2\Sigma_{1/2}$ $(v=0, N=1) \rightarrow A^2\Pi_{1/2}$ $(v'=0, J'=1/2)$, and interact with molecules at a uniform magnetic field. This type of transition will lead to optical pumping into dark ground-state Zeeman sublevels, which could not be excited by the lasers. The states of $F = 2, m = \pm 2$ in the ground state $X^2\Sigma_{1/2}$ $(v=0, N=1)$ are the dark states for MgF. Once there is a dark state, the ground molecular hyperfine state is no longer

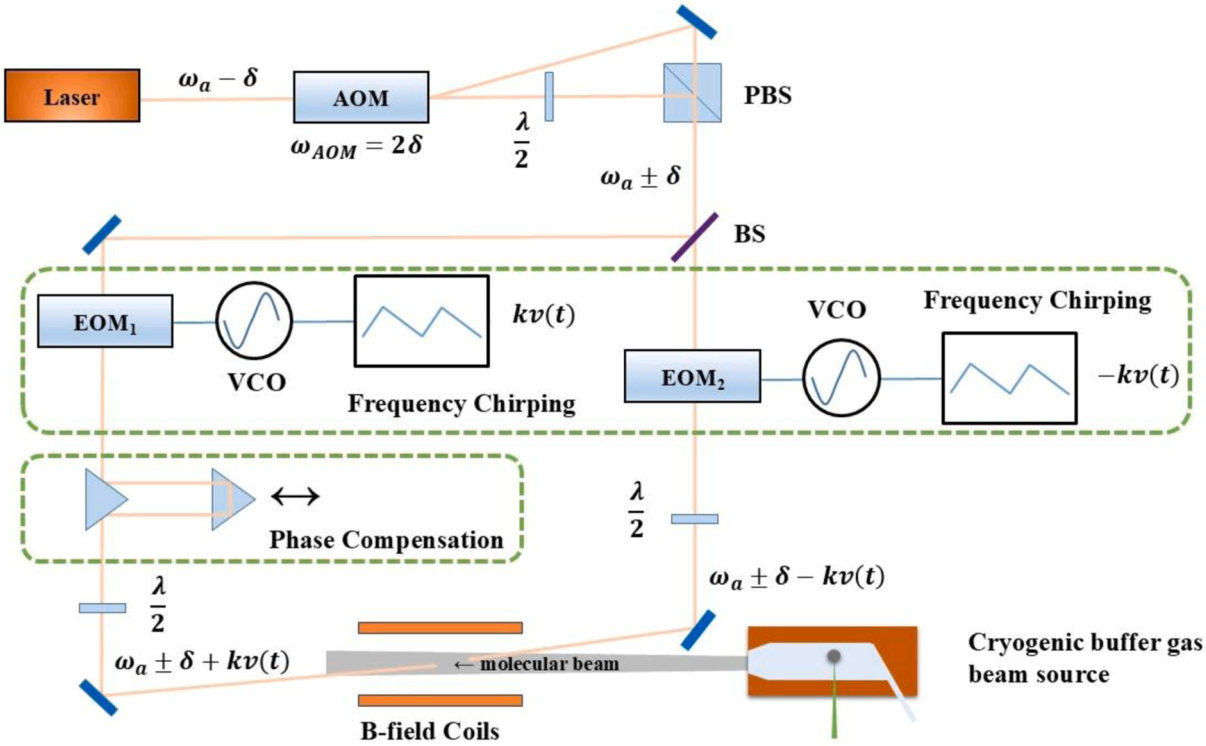

Fig. 2. Proposed scheme of stimulated deceleration of molecules combined with phase compensation and frequency chirping techniques (As shown in the green dashed box). The two counter-propagating travelling-wave lights are π-polarized with the chirped frequency of $\omega_a \pm \delta \pm kv(t)$, and interact with molecules at an optimal angle of a uniform magnetic field. Applying a magnetic field induces the Larmor precession of the molecules, which leads to a periodic exchange of populations of the ground states, so that the molecule will not be trapped in the dark state.

coupled to the excited state by the cooling laser, and the cooling will cease. Applying a magnetic field induces the Larmor precession of the molecules, which leads to a periodic exchange of populations of the ground states, so that the molecule will not be trapped in the dark state. Note that the Larmor precession effect is closely associated with the amplitude of the magnetic field and the angle with the direction of polarized light. The utilization of EOM-based frequency chirping and phase compensation ensures that the maximum force is maintained regardless of the spreading of molecular velocities during deceleration.

2.3. Simulation method

Simulations are valuable in evaluating the performance of the deceleration scheme. And many variable parameters need to be optimized, such as the chirp ramp durations, the chirp magnitude, the magnitude of the applied magnetic field, as well as the laser intensity. Based on the optical Bloch equations model, a 3D Monte-Carlo approach is used to simulate individual molecule trajectories. The physical mechanism of the stimulated force can be effectively described using the π-pulse model [33]. The laser field is oriented along the z-axis. The two components in each laser beam are symmetrically detuned from a carrier frequency ω_a by δ. The total on-axis electric field is:

$$E(z,t) = 2E_0\cos(kz+\omega_a t)\cos(\delta t+\varphi/4) + 2E_0\cos(kz-\omega_a t)\cos(\delta t-\varphi/4), \tag{2}$$

where φ is the phase difference between two standing waves, and $k = 2\pi/\lambda$. With the electric dipole operator $\widehat{d}$ and the amplitude of the Rabi frequency $\Omega_{ij}^0 \equiv E_0\cdot\langle i|\widehat{d}\cdot\widehat{\varepsilon}|j\rangle/\hbar$, the Rabi frequency is:

$$\Omega_{ij}(z,t) = 4\Omega_{ij}^0(\cos(kz)\cos(\delta t)\cos(\varphi/4) + i\sin(kz)\sin(\delta t)\sin(\varphi/4)). \tag{3}$$

The optical Bloch equations of the light field can be derived by considering the motion equation of the density matrix and incorporating the Hamiltonian of the molecules in the optical field [26,33]:

$$\dot{\rho} = \frac{[H,\rho]}{i\hbar} + \left(\frac{d\rho}{dt}\right)_{sp}. \tag{4}$$

application of a magnetic field $\boldsymbol{B}$, at an angle θ relative to the laser polarization. In the following derivation, the summation over the ground state indices *(l, m, n)* runs from 1 to 13, while the summation over the excited state indices *(i, j, k)* runs from 1 to 4. The total Hamiltonian of the system consists of the zero-field Hamiltonian H_0, the Hamiltonian of the interaction between light and the system, and the effective Hamiltonian interacting with the magnetic field H_m [43], which can be expressed as:

$$H\Big/\hbar = H_0\Big/\hbar - \left(\sum_{i,l}\Omega_{e_i g_l}^R|e_i\rangle\langle g_l| + \sum_i \Omega_{e_i d}^R|e_i\rangle\langle d| + c.c\right) + H_m\Big/\hbar, \tag{5}$$

$$H_0\Big/\hbar = \sum_i \omega_{e_i}|e_i\rangle\langle e_i| + \sum_l \omega_{g_l}|g_l\rangle\langle g_l| + \omega_d|d\rangle\langle d|, \tag{6}$$

$$H_m = g_S\mu_B\widehat{S}\cdot\boldsymbol{B}, \tag{7}$$

where $\hbar = h/2\pi$ (h is Planck's constant), $\Omega_{e_i g_l}^R$ and $\Omega_{e_i d}^R$ are the corresponding Rabi frequencies, $|e_i\rangle$ is the excited state, $|g_l\rangle$ is the ground state, and $|d\rangle$ is another state includes all other possible vibrational levels as the total population probabilities are equal to 1. g_S is the electron g-factor and μ_B is the Bohr magneton. The values of the time-dependent density matrix ρ can be obtained by solving the discretized Bloch equations through numerical methods. Assuming that the total decay rate is Γ_i and the decay rate for each channel is Γ_{kl}, the complete density matrix equation of motion for the $M_g + M_e$ system is given by:

$$\dot{\rho}_{e_i e_i} = \sum_m \mathrm{Im}\left[\Omega_{e_i g_m}^*\widetilde{\rho}_{e_i g_m}\right] + \mathrm{Im}\left[\Omega_{e_i d}^*\widetilde{\rho}_{e_i d}\right] - \Gamma_i\rho_{e_i e_i},$$

$$\dot{\rho}_{e_i e_j} = \frac{i}{2}\left[2\left(\omega_{e_j}-\omega_{e_i}\right)\rho_{e_i e_j} - \sum_m\left(\Omega_{e_j g_m}^*\widetilde{\rho}_{e_i g_m} - \Omega_{e_i g_m}\widetilde{\rho}_{e_j g_m}^*\right) - \left(\Omega_{e_j d}^*\widetilde{\rho}_{e_i d} - \Omega_{e_i d}\widetilde{\rho}_{e_j d}^*\right)\right] - \frac{\Gamma_i+\Gamma_j}{2}\rho_{e_i e_j},$$

$$\dot{\widetilde{\rho}}_{e_i d} = \frac{i}{2}\left[2\left(\omega_{ed}^L+\omega_d-\omega_{e_i}\right)\widetilde{\rho}_{e_i d} - \Omega_{e_i d}\left(\rho_{e_i e_i}-\rho_{dd}\right) + \sum_m \Omega_{e_i g_m}\widetilde{\rho}_{d g_m}^* - \sum_{k\neq i}\Omega_{e_k d}\rho_{e_i e_k}\right] - \frac{\Gamma_i}{2}\widetilde{\rho}_{e_i d},$$

In the modelling, λ_{00} is the main slowing light which forms the two-colour light field, and with the repumping light λ_{10} and λ_{21}, the population accumulating in the vibrational states is repumped back. We

$$\dot{\widetilde{\rho}}_{e_i g_l} = \frac{i}{2}\left[2\left(\omega_{eg}^L+\omega_{g_l}-\omega_{e_i}\right)\widetilde{\rho}_{e_i g_l} - \Omega_{e_i g_l}\left(\rho_{e_i e_i}-\rho_{g_l g_l}\right) + \sum_{m\neq l}\Omega_{e_i g_m}\rho_{g_m g_l} - \sum_{k\neq i}\Omega_{e_k g_l}\rho_{e_i e_k} + \Omega_{e_i d}\widetilde{\rho}_{d g_l}\right] - \frac{\Gamma_i}{2}\widetilde{\rho}_{e_i g_l},$$

consider the $M_g = 12+1$ ground states in the MgF molecule. The ground states contain 12 Zeeman sublevels in the $X^2\Sigma_{1/2}^+(v=0, N=1)$ state, and another state includes all other possible vibrational levels as the total population probabilities are equal to 1. There are $M_e = 4$ excited states in the $A^2\Pi_{1/2}$ $(v'=0, J'=1/2)$ state. From Fig. 1, the dark states in the ground state $X^2\Sigma_{1/2}$ $(v=0, N=1)$ are these states of $F = 2, m = \pm 2$ for the π-polarized light. The dark states are destabilized by the

$$\dot{\rho}_{dd} = -\sum_k \dot{\rho}_{e_k e_k} - \sum_m \dot{\rho}_{g_m g_m},$$

$$\dot{\widetilde{\rho}}_{d g_l} = \frac{i}{2}\left[2\left(\omega_{eg}^L+\omega_{g_l}-\omega_{ed}^L-\omega_d\right)\widetilde{\rho}_{d g_l} - \sum_k\left(\Omega_{e_k g_l}\widetilde{\rho}_{e_k d}^* - \Omega_{e_k d}^*\widetilde{\rho}_{e_k g_l}\right)\right],$$

$$\dot{\rho}_{g_l g_l} = \sum_k \left(-\mathrm{Im}\left[\Omega^*_{e_k g_l} \widetilde{\rho}_{e_k g_l}\right] + \Gamma_{kl} \rho_{e_k e_k} \right),$$

$$\dot{\rho}_{g_l g_n} = \frac{i}{2}\left[2(\omega_{g_n} - \omega_{g_l})\rho_{g_l g_n} - \sum_k \left(\Omega_{e_k g_n} \widetilde{\rho}^*_{e_k g_l} - \Omega^*_{e_k g_l} \widetilde{\rho}_{e_k g_n} \right) \right],$$

$$\widetilde{\rho}_{e_i g_l} = \rho_{e_i g_l} e^{i\omega^L_{eg} t},$$

$$\widetilde{\rho}_{e_i d} = \rho_{e_i d} e^{i\omega^L_{ed} t},$$

$$\widetilde{\rho}_{d g_l} = \rho_{d g_l} e^{i\left(\omega^L_{eg} - \omega^L_{ed}\right)t}. \tag{8}$$

The force acting on a molecule is equal to the negative gradient of the interaction potential [26,33], which is given by

$$\langle \widehat{F} \rangle = -\langle \nabla \widehat{H} \rangle = -Tr(\rho \nabla \widehat{H}). \tag{9}$$

The phase difference between two standing waves can be expressed as:

$$\varphi = 2\chi, \tag{10}$$

$$\chi = 2\delta \cdot z/c, \tag{11}$$

where χ is the phase difference between the electric fields of the counterpropagating beat notes and z is the position of the molecule. The molecule transitions from an excited state to a ground state through either stimulated or spontaneous radiation. The average stimulated force is zero if the beat notes are evenly distributed in time with the spontaneous radiation process. By adjusting the phase difference between opposite beats, the occurrence of spontaneous radiation can be reduced and the optimal stimulated force shape can be achieved, which we call as phase compensation. Equation (3) shows that the frequency detuning significantly influences the stimulated interaction between the light field and the molecules. The magnitude of the stimulated force acting on MgF molecules increases with δ; however, the required laser power scales with δ^2. Note that requiring the high-power laser light presents a significant challenge in actual experiments, especially when the detuning is several hundred times the natural linewidth γ.

The aim is to decelerate MgF molecules in the presence of an optical field, achieving a velocity below 20 m/s. The deceleration process in MgF induces a Doppler shift relative to the optical field, resulting in frequencies in the hundreds of megahertz range that rapidly change as the molecule velocity decreases. At a molecule velocity of 220 m/s relative to the light field, the Doppler shift is 612.3 MHz. This large Doppler shift greatly affects the process of stimulated cycling. Fig. 3 shows that the amplitude of the stimulated forces on the MgF molecules decreases significantly as Doppler shift $\Delta\omega$ changes when the detuning is 15γ. The Doppler shift is 167 MHz at a molecule velocity of about 60 m/s. When the Doppler shift exceeds 200 MHz, the forces experienced by the molecules are close to zero. This indicates a significant impact of molecular speed on the stimulated radiation cycle between light and molecules.

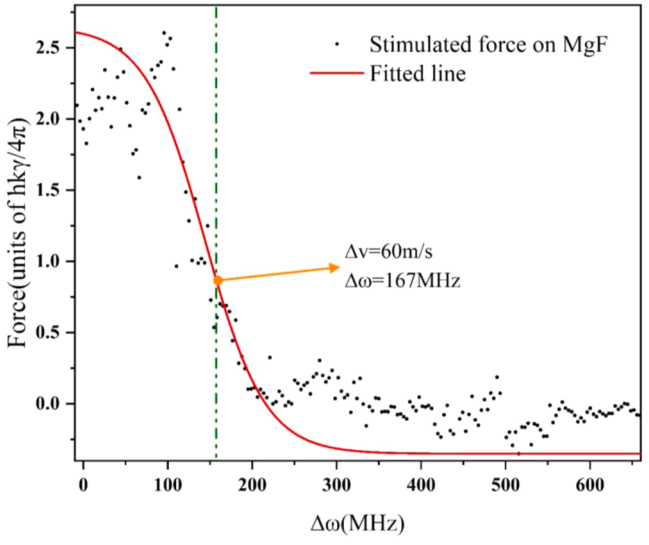

Fig. 3. Variation of stimulated forces under the Doppler shift ranging from 0 MHz to 650 MHz. The black points represent the calculated forces on MgF molecules, and the solid red curve indicates the fitting by Boltzmann function. The green vertical dashed line shows that the Doppler shift is 167 MHz at a molecular velocity of about 60 m/s.

The phase compensation enables the maintenance of an optimal shape for the stimulated force. The force is sizable only within the velocity range $|v| < \delta/2k$, and the initial velocity distribution of molecules is typically wide, so the forces experienced by molecules during deceleration are inherently non-uniform. The conventional stimulated force generated by the interaction between the laser field and molecules exhibits the inhomogeneous distribution in both spatial and frequency domains. These issues greatly hinder laser deceleration efficiency and ultimately decrease the number of slowed molecules.

To solve the above issues, synchronous frequency chirping is employed to maintain the continuous action of the stimulated cycle by tracking the velocity of slowing MgF molecules. The use of frequency chirping is essential to ensure that almost all molecules with different velocities are fully decelerated to the velocity that satisfies the MOT capture velocity range, thereby greatly increasing the number of molecules loaded in the MOT. The laser frequency is chirped by the EOM:

$$\omega(t) = \omega_a \pm \delta \pm \boldsymbol{k} \cdot \boldsymbol{v}(t). \tag{12}$$

In Monte-Carlo simulation, we search and locate the three-dimensional positions and velocities of the molecules within a unit of time $\sim 10^{-6}$ s, and then determine the variations in parameters, such as the real-time mean force, relative frequency and acceleration of the molecules. Finally, we statistically estimate the number of molecules positioned at the MOT site.

3. Result and discussion

3.1. Stimulated force on MgF

The dark Zeeman sublevels are a significant problem in laser cooling of molecules. Our study in 2021 shows that the dark states in MgF are forced to Larmor process into the bright states by applying an external magnetic field [42]. Fig. 4(a) investigates the effect of the magnetic field in terms of the magnitude and angle on the average stimulated forces at near zero velocities for the purpose of remixing the dark states in a π-polarized laser field. From the 3D plot, it is clear that an excessive magnetic field with improper angle disrupts the original coupling mechanism of molecular energy levels, significantly impacting the stimulated radiation cycle and reducing the force magnitude. Fig. 4(b) shows the stimulated forces for $B = 25$ G and $\theta = 65^\circ$ as the detuning changes. The force magnitude and velocity range decrease as the detuning decreases, resulting in a shorter and weaker interaction between the laser and the molecules. For δ values of 10γ, 15γ, and 20γ, the corresponding laser irradiance for each travelling wave is 56.2 W/cm^2, 126.3 W/cm^2, and 224.7 W/cm^2, respectively. As the laser power increases, the velocity capture range of $\delta/2k$ expands to the values of approximately 39.7 m/s, 59.6 m/s, and finally up to 79.4 m/s. Thus, decreasing the laser intensity causes a reduction of the stimulated force magnitude and an increase in the spatial non-uniformity.

During the interaction between the light field and the molecules, the beat phase difference ($\chi = 2\delta \cdot z/c$) varies with the molecules' spatial position. As the molecular beam moves, the beat phase difference strongly influences the magnitude of the stimulated force during the

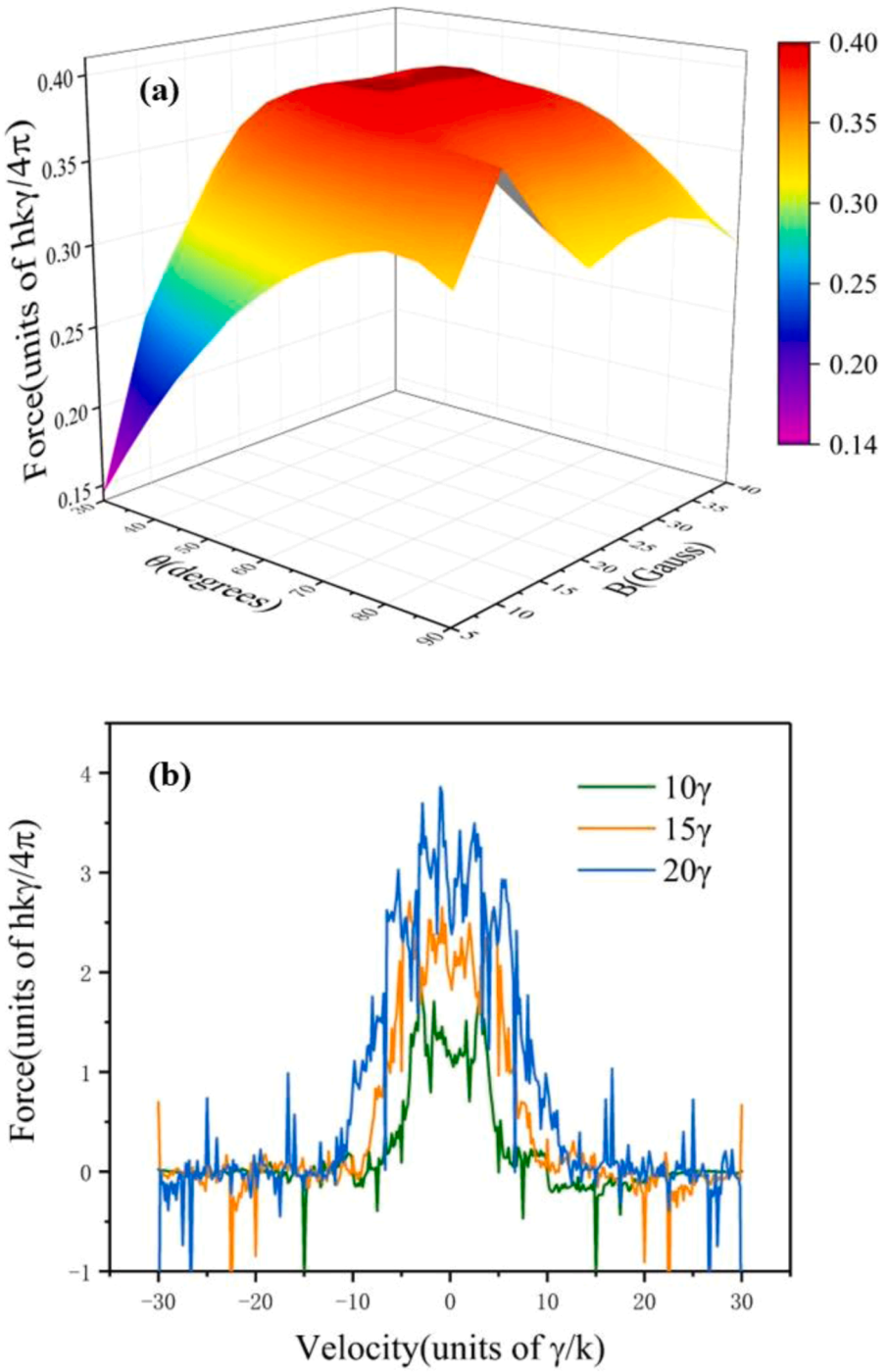

Fig. 4. (a) Stimulated forces at near-zero molecular velocities as a function the magnetic field in angle and magnitude, δ is fixed at 10γ. (b) Stimulated forces as a function of molecular velocity at different detune frequencies; the magnetic field is fixed 25 G.

deceleration. To investigate the variation trend, we calculate the force-velocity curves for beat phase differences from 45° to 75° in an increment of 2°, as shown in Fig. 5. The result shows that the force magnitude rapidly decreases with the change of beat phase difference over a short distance of several centimetres. The blue curve shows the calculated forces on MgF molecules, and each curve in the figure represents a distinct force profile at a specific beat phase difference. To illustrate the variation in force amplitude with different phase differences, the force near zero velocity is marked with an orange curve in Fig. 5. A 26.4° change in the phase difference can cause a rapid decrease in the force, even when the deceleration distance is only 1 cm. The absorption-stimulated emission cycles can maintain the optimal shape and magnitude of the stimulated forces on molecules only if the phase difference remains stable at $\chi = 45°$ during deceleration. However, even under optimal phase conditions, an inhomogeneous distribution of average forces during deceleration can significantly reduce the efficiency of molecular deceleration. Therefore, EOM-based frequency chirping and phase compensation are employed in the next for efficient stimulated force deceleration of MgF molecules.

3.2. Deceleration of mgf molecular beam

The frequency chirping technique allows for maintaining the maximum stimulated force to be applied to the entire molecular velocity

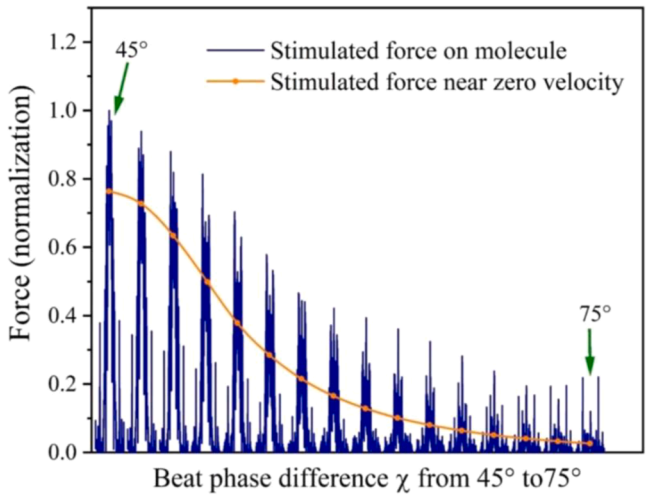

Fig. 5. Stimulated forces vary with beat phase difference changing from 45° to 75° in a deceleration distance of 2.3 cm. The blue curve shows the calculated forces on MgF molecules and the orange curve represents the trend of the average forces near zero velocity.

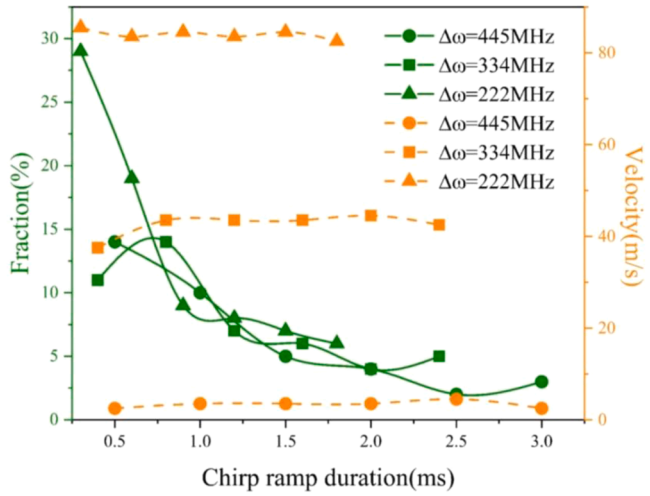

Fig. 6. Comparison of the deceleration results in different chirp magnitudes $\Delta\omega$ and chirp ramp durations at a laser power of 441.1 mW. The MgF molecular beam has an initial $v = (200 \pm 50)$ m/s. The dashed curves show the final longitudinal velocity after deceleration. The solid curves show the deceleration efficiency of the molecules. We count the number of the slowed molecules in the detection range. The fraction is expressed by dividing the number of the slowed molecules by the initial one million. Thus, the final number of detected molecules is lower than the initial number due to transverse diffusion during deceleration.

distribution throughout the deceleration process. Fig. 6 shows the comparison of the deceleration results obtained with varying chirp magnitudes and chirp ramp durations, with a detuning of 10γ and laser power of 441.1 mW per travelling wave beam. The molecular beam from a buffer gas source has a forward velocity distribution centred at 200 m/s with a full width at half maximum (FWHM) of 100 m/s. The FWHM of the transverse velocity distribution is fixed at 2 m/s after the molecules pass through the collimation aperture [43]. Fig. 6 shows that when the chirp amplitude $\Delta\omega$ is at 222 MHz, although the overall number of slowed MgF molecules are relatively high, the longitudinal velocity of the slowed molecules exceeds 80 m/s. This does not meet the requirements for velocity of molecules to being able to be captured by a MOT. As the chirp ramp duration increases, the number of slowed molecules decreases, while the final velocity remains essentially stable.

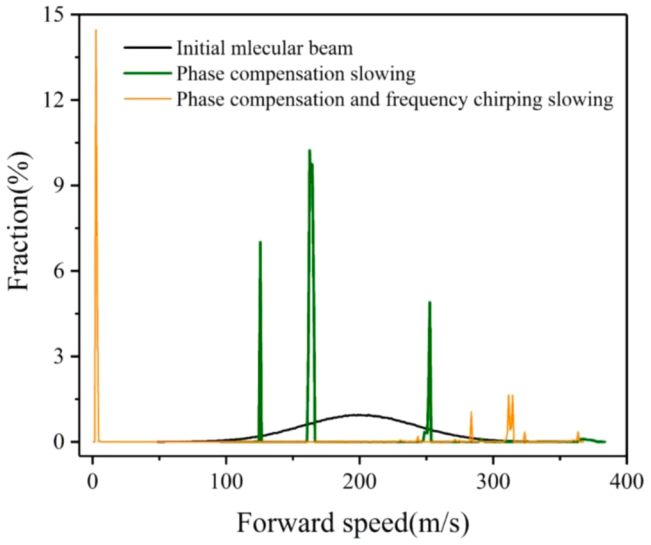

Fig. 7. Two different schemes are employed to achieve deceleration of the MgF molecular beam under a detuning of 10γ and laser power of 441.1 mW per travelling wave beam. Scheme (a) (the green curve) involves deceleration with a constant beat phase difference of $\chi = \pi/4$, only utilizing phase compensation. Scheme (b) (the orange curve) utilizes both phase compensation and frequency chirping for deceleration. The black curve represents the initial velocity distribution of the molecules.

When the chirp magnitude $\Delta\omega$ is at 334 MHz, the number of decelerated slow molecules increases with the chirp ramp duration initially, reaches its maximum at about 1.0 ms, and then begins to decline as the duration is further extended. When the chirp magnitude $\Delta\omega$ is at 445 MHz, the final velocity of the molecules remains stable below 10m/s, which is good news to further work on trapping of MgF molecules.

Throughout the deceleration process, loss of molecules is inevitable because of the transverse diffusion. A free flight and deceleration process are involved in a complete slowing sequence. After slowing is finished, molecules arrive at the position of an MOT. In addition, only molecules passing within a 10 mm diameter circle centred on the z axis are counted. Such a setup is reasonable because trapping force approximately peaks at a displacement of 10 mm in a typical molecular MOT, being sufficient to load a molecular beam with a diameter of 10 mm. We have performed Monte-Carlo simulations for one million molecules of MgF using two different deceleration schemes, and count the number of the slowed molecules in the detection range.

Fig. 7 shows the velocity distribution of the molecules at the detecting distance 11 cm from the exit of the buffer gas cell, and the black curve represents the initial velocity distribution of the molecules without laser slowing. Phase compensation is used to maintain the best force profile, as the molecules pass through the optical field. The beat phase difference is $\pi/4$. The detuning is 10γ. The magnetic field magnitude is 25 G and its angle is 65°. We count the number of the slowed molecules in the detection range. The fraction is expressed by dividing the number of the slowed molecules by the initial one million. The final number of detected molecules is lower than the initial number due to transverse diffusion during deceleration. The green solid curve in Fig. 7 shows that three slices of the molecular beam are decelerated due to the narrow velocity capture range of the stimulated force at this light intensity, which is only 39.7 m/s. Using frequency chirping and phase compensation, the orange curve in Fig. 7 shows that fast molecules can be decelerated to 2.5 m/s using a 445 MHz chirp with a ramp duration of 500 μs. The fraction of slowed molecules at 2.5 m/s is 14.5 %, meaning that 14.5 % of the slowed MgF molecules are decelerated to velocities below 10 m/s, within the MOT capture velocity range. A laser power of 441.1 mW with a frequency chirp of 445 MHz provides a needed slowing of $25.3\gamma/k$ (velocity range of 200 m/s). The deceleration of the MgF

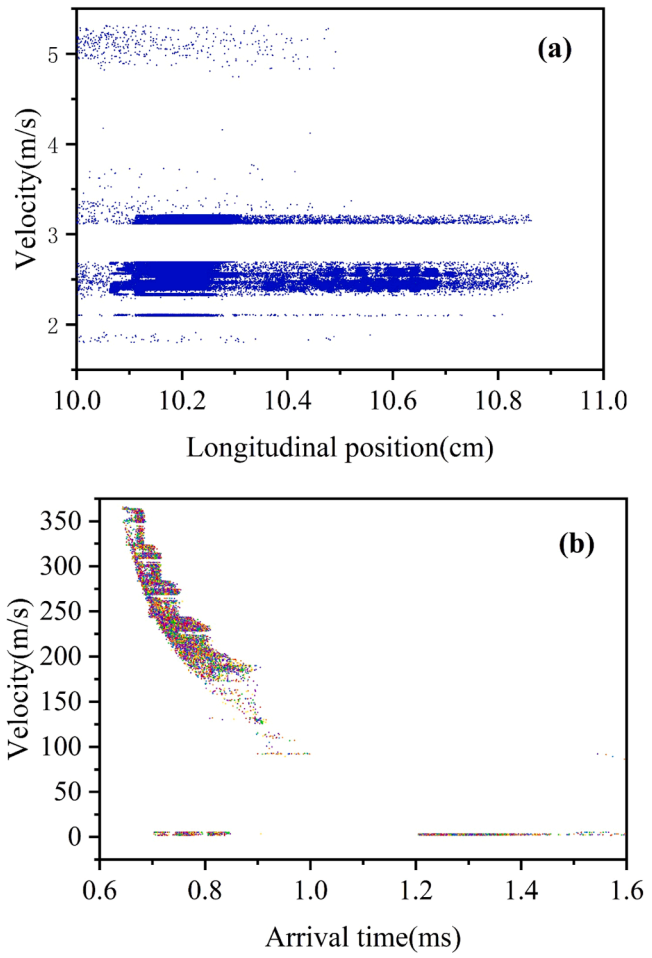

Fig. 8. The velocity distribution and arrival times of one million molecules after deceleration. (a) Velocity distribution of MgF molecules with position after laser-slowing is completed, shown by the blue dots. (b) Arrival time and forward velocity of MgF molecules that reach the MOT position, shown by the colourful dots.

molecules at faster velocity has also been achieved, resulting in a remarkable 55.6 % reduction in laser power requirements [36]. And the required laser power for MgF is only 44.7 % of that for CaF [33].

Parameters for a typical buffer-gas-cooled molecular beam are as follows: the exit aperture of the buffer gas cell has a diameter of 3–5 mm to extract a precooled molecular beam, and a 1.5 mm × 1.5 mm aperture is used to further collimate the molecular beam for deceleration and cooling [44], which results in a steradian of 1.9×10^{-4} [43]. If the flux of MgF from a buffer gas chamber is $2 \times 10^{11} \sim 10^{12}$ per steradian per molecular pulse in the ground state [20,45], we can estimate the number of slowed MgF molecules that satisfy a typical MOT capture velocity range. For a CaF MOT, it has been demonstrated that the number of molecules to be trapped is approximately half the number that are within the capture velocity and capture volume [45]. We assume the similar parameters for the MgF MOT. To investigate the deceleration dynamics of all molecules, we analysed the velocity distribution and arrival times of one million molecules after deceleration, as shown in Fig. 8. We performed a Monte-Carlo simulation with one million MgF molecules. After the deceleration process, the molecules within the detection range were counted. Fig. 8(a) shows the molecular phase-space distribution within the capturable velocity range of the MOT. As shown in Fig. 8(a), each point represents the position and velocity of a single molecule. Due to the high density and large number of points, a "discrete final velocity streaks" effect is observed. In fact, a significant portion of the MgF molecules have velocities around 2.5 m/s, while many others have velocities around 2 m/s and 3.2 m/s, with a smaller fraction reaching around 5 m/s. In Fig. 8(b), the points in the upper-left region indicate molecules with fast velocities that reach the MOT region in a shorter time, and they can't be captured by the MOT. As the molecules interact with the light field, the fraction of molecules is effectively decelerated, allowing the slower MgF molecules to be captured by the MOT. The molecules with lower initial velocities take longer to travel, resulting in a longer arrival time at the MOT location after deceleration. Fig. 8 illustrates that the slow molecules arrive at the MOT location, 11 cm from the buffer gas cell, for a period of about 1.6 ms. The spatial distribution of molecules within 1 cm after deceleration indicates that approximately $5 \times 10^6 \sim 10^7$ MgF molecules can be confined in the MOT, which is at least one order of magnitude higher than that achieved through the radiative force [46]. This improvement can be attributed to the powerful stimulated force based on the combination of phase compensation and frequency chirping.

Furthermore, the deceleration of MgF at laser powers of 441.1 mW, 992.6 mW and 1764.6 mW, respectively, is also simulated. The molecular beam has an initial velocity of (200 ± 50) m/s and a free-flight distance of 5 cm before deceleration. The tightly focused laser beams with a top-hat diameter of 1 mm are used to achieve the required irradiance [26,34]. As shown in Table 1, a reduction in laser power will result in a decrease in the velocity range of the stimulated force, resulting in an inhomogeneous force distribution. This is due to the fact that the force is only sizable for velocities less than $\delta/2k$ during deceleration. Scheme (a) shows that it decelerates molecules using phase compensation to maintain a stable stimulated force profile. However, even with a laser power of 1764.6 mW, Scheme (a) is only capable of slowing the molecules to a speed of over 60 m/s. In other words, a much higher laser power is required to decelerate the buffer gas-cooled MgF molecules to be within the MOT capture velocity range. Scheme (b) involves the deceleration utilizing both phase compensation and frequency chirping. With a laser power of only 441.1 mW, MgF molecules can be effectively decelerated from a forward velocity of 200 m/s to 2.5 m/s. The final velocity of MgF molecules in Scheme (b) is much smaller than that of the molecules in Scheme (a). These results will be applicable to the investigation of stimulated deceleration in heavy molecular systems under low laser power.

Table 1
The results from Monte-Carlo simulations for two deceleration schemes on MgF molecules with varying detuning and laser power. Scheme (a) employs deceleration through phase compensation. Scheme (b) employs a combination of phase compensation and frequency chirping for deceleration.

Detuning (MHz)	10γ		15γ		20γ	
Irradiance (W/cm^2)	56.2		126.3		224.7	
Laser power per beam (mW)	441.1		992.6		1764.6	
Velocity range (m/s)	39.7		59.6		79.4	
Scheme	(a)	(b)	(a)	(b)	(a)	(b)
Final velocity (m/s)	162.5	2.5	87.5	2.5	62.5	2.5

3.3. Synchronous stimulated deceleration of heavy molecules

Polar heavy-atom molecules are frequently regarded as optimal candidates for precision measurements and tests of fundamental physics. They are superior to atoms for measuring electron electric dipole moments (eEDMs) due to their stronger polarization, which enhances interaction with the eEDM and reduces systematic errors from magnetic fields and geometric phases [47–49]. The first molecular determination of the eEDM with YbF gave an upper limit of approximately 10^{-28} e cm [47]. According to a recent study by Alauze et al. in 2021, the current molecular beam generated from a cryogenic buffer-gas source would require an experiment spanning over 1.5 m for efficient utilization of these ultra-cold molecules, despite a mean forward speed ranging from 160 m/s to 220 m/s [48]. Taking YbF molecules as an example, the

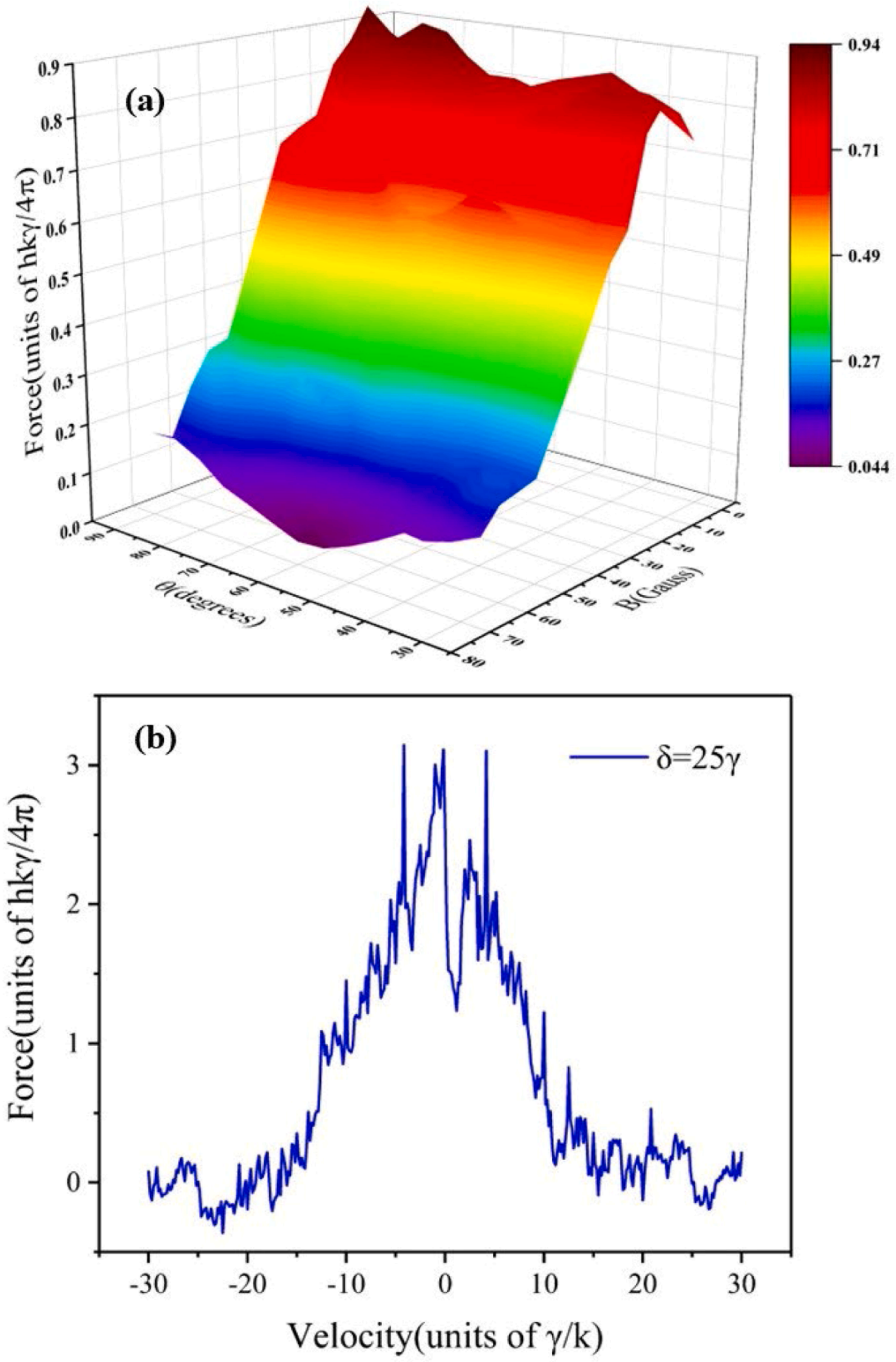

Fig. 9. (a) Plot of the stimulated forces as a function of magnetic field magnitude and angle on the average stimulated forces at near-zero velocities of YbF molecules for a π-polarized laser field in order to manipulate dark states. (b) The stimulated force on YbF molecule for the $X^2\Sigma_{1/2}$ $(v=0, N=1) \rightarrow A^2\Pi_{1/2}$ $(v'=0, J'=1/2)$ at $\delta = 25\gamma$.

parameters are: the initial forward velocity is 200 m/s with an FWHM of 100 m/s at the laser power of 210.9 mW per travelling wave. Tightly focused laser beams with a top-hat diameter of 1 mm is used to achieve the required irradiance. Applying our scheme(b) shows that an YbF cryogenic buffer-gas beam can be decelerated down to a velocity of 2.5 m/s by using a stimulated deceleration scheme within a distance of <10 cm.

The amplitude of the stimulated forces decreases as the magnetic field strength increases, as depicted in Fig. 9(a). The time-dependent density matrix of a multilevel system of YbF molecule is numerically solved with the rotating-wave approximation at 552 nm with a natural linewidth of $\gamma = 2\pi \times 5.7$ MHz, and the stimulated force on molecules is shown in Fig. 9(b). A static magnetic field with a magnitude of 10 G and an angle of 75° is applied to remix the Zeeman dark states, which are characterized by $m_F = \pm 2$ in the ground state of $F = 2$.

The green solid curve in Fig. 10 shows that YbF molecules with initial forward of 200 m/s are decelerated to several slicing beams using the phase compensation scheme. They are fast molecules of over 100 m/s. The final number of counted molecules is lower than the initial number due to transverse diffusion during deceleration. As shown in the orange solid curve in Fig. 10, the synchronous deceleration method is employed with a laser power of 210.9 mW per traveling wave, resulting in the

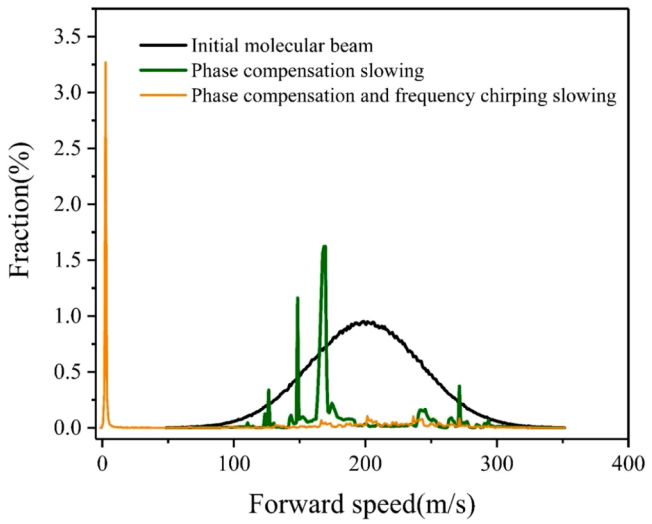

Fig. 10. The initial and final velocity distributions of YbF molecules with two different schemes under the laser power of 210.9 mW per travelling wave beam. The green curve shows the deceleration with phase compensation and the orange curve represents the slowing with both phase compensation and frequency chirping for deceleration. The fraction is expressed by dividing the number of the slowed molecules in the detection range by the initial one million, and the final number of detected molecules is lower than the initial number due to transverse diffusion during deceleration.

effective slowing of the molecules to a velocity below 5 m/s. The fraction of slowed molecules at 2.5 m/s is 3.3 %, meaning that 3.3 % of the slowed YbF molecules are decelerated synchronously to velocities within the MOT capture velocity range. The combination of phase compensation with frequency chirping provides a powerful stimulated force, which ensures rapid and efficient deceleration of fast YbF molecules. This is due to the peak force coinciding with the molecular motion. In contrast to the deceleration method employed with heavy molecules with an initial velocity of 120 m/s, the laser power requirement has decreased by nearly 80 % [37].

The previous sections have shown that as laser power increases, both the maximum stimulated force and velocity range also increase. In the case of heavy-atom molecules such as YbF, the deceleration efficiency is influenced by the initial longitudinal velocity at a given laser power and magnetic field magnitude. We analysed the velocity distribution and arrival times of one million YbF molecules after deceleration. As shown in Fig. 11, slow molecules arrive at the MOT location, which is 16.5 cm from the buffer gas source, for a duration of about 1.6 ms. We are able to achieve a synchronous deceleration on YbF molecular beam in 5 cm distance as shown by the blue dots in Fig. 11(a). And the longitudinal velocity distribution of the molecules is effectively compressed within a range of 5 m/s, compared to the initial width before deceleration, resulting in efficient cooling. The observed longitudinal phase-space distribution after deceleration indicates that slowed molecules are distributed over a region approximately 5 cm in width. As indicated by the colourful dots in the Fig. 11(b), the molecules whose velocities are over hundreds of meters per second, rapidly reach the detection area at around 1.1 ms, while slower molecules also arrive within 0.5 ms. In short, the extremely short deceleration time significantly minimizes the loss of the molecules caused by lateral diffusion during flight. The flux of YbF emitted from a cryogenic buffer gas cell in a single internal state is 10^{10} per steradian per pulse [48]. Our estimate of the number of captured molecules is 3×10^6 in the MOT.

Monte-Carlo simulations of molecule deceleration using stimulated force based on the combination of phase compensation and frequency chirping are shown in Table 2. We also include results for both light and heavy polar molecules; both types of molecules are efficiently decelerated to meet the requirements of MOT capture velocity range at a low

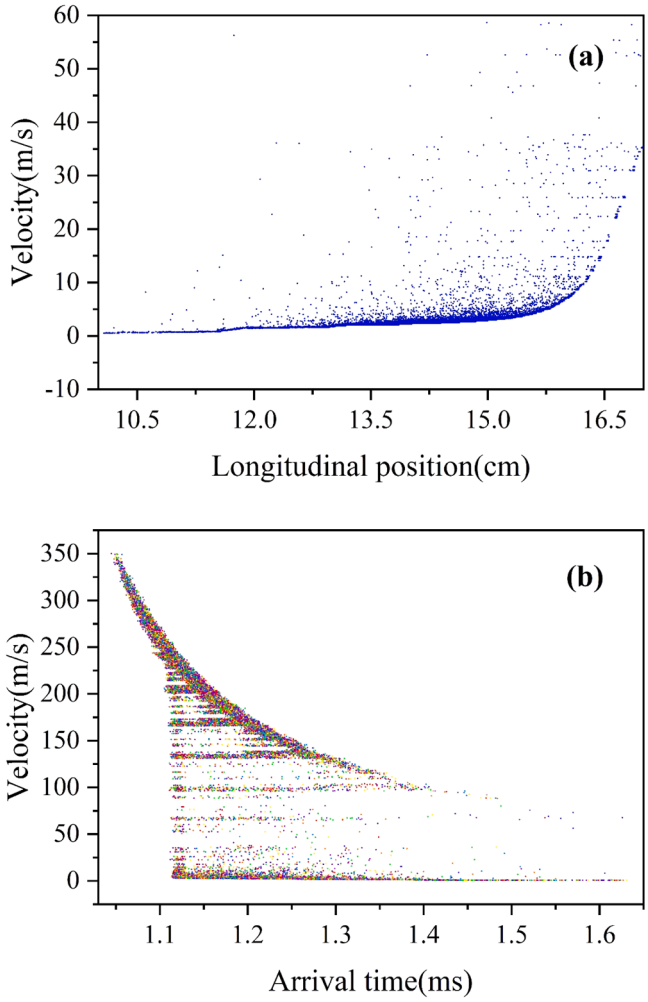

Fig. 11. The velocity distribution and arrival times of one million molecules after deceleration. (a) Longitudinal velocity distribution of YbF molecules with position after slowing, shown by the blue dots. (b) Arrival time and forward velocity of YbF molecules that arrive at the MOT position, shown by the colourful dots.

Table 2
Parameters and results in Monte-Carlo simulations of stimulated deceleration on MgF molecules and YbF molecules.

	MgF	YbF
Mass (amu)	43	193
Wavelength (nm)	359	552
Natural linewidth (MHz)	$2\pi \times 22.1$	$2\pi \times 5.7$
Laser power per beam (mW)	441.1	210.9
Magnetic field magnitude (G)	25	10
Magnetic field angle (°)	65	75
Velocity range (m/s)	39.7	39.3
Initial forward speed (m/s)	200	200
Final forward speed (m/s)	2.5	2.5
Deceleration efficiency	14.5 %	3.3 %

laser power. As revealed from the table, this slowing process is strongly influenced by the wavelength and the upper state lifetime of the molecule. Although YbF has ~ 4.5 times the molecular mass of MgF, the latter has a higher value of $\lambda/2\pi\tau$, which is 2.5 times larger than that of YbF. At a final forward velocity of 2.5 m/s, the deceleration efficiency of MgF molecules exceeds that of YbF by a factor of four. The contribution of spontaneous radiation must be considered in the interaction between light fields and molecules. The shorter the duration of a molecule is in its

excited state, the lower the probability of spontaneous radiation is occurring. However, when a molecule transitions to another radiation cycle, its duration in the excited state increases, thereby increasing the probability of spontaneous radiation. The magnitude of the final net force on the molecule is then reduced. Therefore, it is desirable for the molecule to undergo more of the same absorption-stimulated emission cycles before a spontaneous emission occurs.

4. Conclusion

Theoretical studies have been conducted to illustrate the stimulated force deceleration of polar molecules MgF (light) and YbF (heavy). This has been achieved by maintaining a synchronous, constant maximum force on molecules using the low-power laser light, with a phase compensation and frequency chirping. The numerical model and Monte-Carlo simulations analyse the stimulated force deceleration of molecules under realistic experimental conditions. The main new results are summarized as below:

(1) This study demonstrates the benefits of using phase compensation and frequency chirping to maintain an optimal stimulated force on molecules, thereby reducing the high laser power required for conventional stimulated deceleration. A cryogenic buffer-gas beam of MgF molecules with an initial velocity of 200 m/s can be effectively decelerated to below 10 m/s with a laser power of 441.1 mW, which represents a 55.6 % reduction in laser power requirement [36]. And the required laser power for MgF is only 44.7 % of that for CaF [33]. The estimated number of molecules that can be confined in an MOT is $5 \times 10^6 \sim 10^7$. This is at least one order of magnitude higher than the number of molecules decelerated by resonant radiation force [46].

(2) A cryogenic buffer-gas beam of YbF molecules with an initial forward velocity of 200m/s can be decelerated to the velocity of 2.5 m/s by using the similar scheme, at a laser power of 210.9 mW per travelling wave. This method requires approximately 80 % less power than the conventional deceleration of YbF with an initial velocity of 120 m/s and a final velocity of 5.7 m/s [37]. The estimated number of YbF molecules captured in the MOT is 3×10^6.

(3) The effectiveness of the stimulated deceleration mechanism is strongly influenced by the molecular properties, specifically the lifetime of the upper state and the wavelength associated with the cooling transition. To ensure the maintenance of a robust deceleration force, it is advantageous for the molecule to undergo the same multiple absorption-stimulated emission sequences prior to the occurrence of spontaneous emission. Decelerating molecules with lower power light not only overcomes the problems of high laser power requirements and inhomogeneous stimulated force distribution, but also increases the number of molecules that can be loaded into a MOT. This allows the optical deceleration and loading of a wide range of dense, ultracold molecular species into a MOT for evaporative cooling to quantum degeneracy [50–52]. Such theoretical results are important for future experimental consideration.

CRediT authorship contribution statement

Jin Wei: Writing – review & editing, Writing – original draft, Methodology, Investigation, Formal analysis, Data curation. **Di Wu:** Investigation. **Taojing Dong:** Investigation. **Chenyu Zu:** Investigation. **Tao Yang:** Supervision. **Yong Xia:** Writing – review & editing, Writing – original draft, Supervision, Methodology, Investigation, Funding acquisition, Data curation, Conceptualization. **Jianping Yin:** Supervision.

Declaration of competing interest

The authors declare that they have no known competing financial interests or personal relationships that could have appeared to influence the work reported in this paper.

Acknowledgements

This work is financially supported by the National Natural Science Foundation of China (12174115, 12274140, 91836103).

Data availability

Data will be made available on request.

References

[1] Y.C. Bao, S.S. Yu, L. Anderegg, E. Chae, W. Ketterle, K.-K. Ni, J.M. Doyle, Dipolar spin-exchange and entanglement between molecules in an optical tweezer array, Science 382 (2023) 1138.
[2] C.M. Holland, Y. Lu, L.W. Cheuk, On-demand entanglement of molecules in a reconfigurable optical tweezer array, Science 382 (2023) 1143.
[3] T. Karman, M. Tomza, J. Pérez-Ríos, Ultracold chemistry as a testbed for few-body physics, Nat. Phys. 20 (2024) 722–729.
[4] D. DeMille, J.M. Doyle, A.O. Sushkov, Probing the frontiers of particle physics with tabletop-scale experiments, Science 357 (2017) 990.
[5] L.D. Carr, D. DeMille, R.V. Krems, J. Ye, Cold and ultracold molecules: science, technology and applications, New J. Phys. 11 (2009) 055049.
[6] J.F. Barry, D.J. McCarron, E.B. Norrgard, M.H. Steinecker, D. DeMille, Magneto-optical trapping of a diatomic molecule, Nature 512 (2014) 286.
[7] L. Anderegg, B.L. Augenbraun, E. Chae, B. Hemmerling, N.R. Hutzler, A. Ravi, A. Collopy, J. Ye, W. Ketterle, J.M. Doyle, Radio frequency magneto-optical trapping of CaF with high density, Phys. Rev. Lett. 119 (2017) 103201.
[8] S. Truppe, H.J. Williams, M. Hambach, L. Caldwell, N.J. Fitch, E.A. Hinds, B. E. Sauer, M.R. Tarbutt, Molecules Cooled Below the Doppler Limit 13 (2017) 1173. Nat. Phys.
[9] A.L. Collopy, S. Ding, Y. Wu, I.A. Finneran, L. Anderegg, B.L. Augenbraun, J. M. Doyle, J. Ye, 3D Magneto-optical trap of yttrium monoxide, Phys. Rev. Lett. 121 (2018) 213201.
[10] Z.X. Zeng, S.H. Deng, S.K. Yang, B. Yan, Three-dimensional magneto-optical trapping of barium monofluoride, Phys. Rev. Lett. 133 (2024) 143404.
[11] N.B. Vilas, C. Hallas, L. Anderegg, P. Robichaud, A. Winnicki, D. Mitra, J.M. Doyle, Magneto-optical trapping and sub-doppler cooling of a polyatomic molecule, Nature 606 (2022) 70.
[12] L. Anderegg, B.L. Augenbraun, Y. Bao, S. Burchesky, L.W. Cheuk, W. Ketterle, J. M. Doyle, Laser cooling of optically trapped molecules, Nat. Phys. 14 (2018) 890.
[13] D.J. McCarron, M.H. Steinecker, Y. Zhu, D. DeMille, Magnetic trapping of an ultracold gas of polar molecules, Phys. Rev. Lett. 121 (2018) 013202.
[14] H.J. Williams, L. Caldwell, N.J. Fitch, S. Truppe, J. Rodewald, E.A. Hinds, B. E. Sauer, M.R. Tarbutt, Magnetic trapping and coherent control of laser-cooled molecules, Phys. Rev. Lett. 120 (2018) 163201.
[15] L. Anderegg, L.W. Cheuk, Y. Bao, S. Burchesky, W. Ketterle, K.-K. Ni, J.M. Doyle, An optical tweezer array of ultracold molecules, Science 365 (2019) 1156.
[16] J.J. Burau, P. Aggarwal, K. Mehling, J. Ye, Blue-detuned magneto-optical trap of molecules, Phys. Rev. Lett. 130 (2023) 193401.
[17] M.R. Tarbutt, T.C. Steimle, Modeling magneto-optical trapping of CaF molecules, Phys. Rev. A 92 (2015) 053401.
[18] J.F. Barry, E.S. Shuman, E.B. Norrgard, D. DeMille, Laser radiation pressure slowing of a molecular beam, Phys. Rev. Lett. 108 (2012) 103002.
[19] B. Hemmerling, E. Chae, A. Ravi, L. Anderegg, G.K. Drayna, N.R. Hutzler, A. L. Collopy, J. Ye, W. Ketterle, J.M. Doyle, Laser slowing of CaF molecules to near the capture velocity of a molecular MOT, J. Phys. B 49 (2016) 174001.
[20] S. Truppe, H.J. Williams, N.J. Fitch, M. Hambach, T.E. Wall, E.A. Hinds, B.E. Sauer, M.R. Tarbutt, An intense, cold, velocity-controlled molecular beam by frequency-chirped laser slowing, New J. Phys. 19 (2017) 022001.
[21] M. Yeo, M.T. Hummon, A.L. Collopy, B. Yan, B. Hemmerling, E. Chae, J.M. Doyle, J. Ye, Rotational state microwave mixing for laser cooling of complex diatomic molecules, Phys. Rev. Lett. 114 (2015) 223003.
[22] P. Kaebert, M. Stepanova, T. Poll, M. Petzold, S. Xu, M. Siercke, S. Ospelkaus, Characterizing the zeeman slowing force for CaF molecules, New J. Phys. 23 (2021) 093013.
[23] K.J. Rodriguez, N.H. Pilgram, D.S. Barker, S.P. Eckel, E.B. Norrgard, Simulations of a frequency-chirped magneto-optical trap of MgF, Phys. Rev. A 108 (2023) 033105.
[24] C. Zhang, S.T. Rittenhouse, T.V. Tscherbul, H.R. Sadeghpour, N.R. Hutzler, Sympathetic cooling and slowing of molecules with Rydberg atoms, Phys. Rev. Lett. 132 (2024) 033001.
[25] H. Metcalf, Colloquium: strong optical forces on atoms in multifrequency light, Rev. Mod. Phys. 89 (2017) 041001.

[26] S.E. Galica, L. Aldridge, D.J. McCarron, E.E. Eyler, P.L. Gould, Deflection of a molecular beam using the bichromatic stimulated force, Phys. Rev. A 98 (2018) 023408.
[27] I. Kozyryev, L. Baum, L. Aldridge, P. Yu, E.E. Eyler, J.M. Doyle, Coherent bichromatic force deflection of molecules, Phys. Rev. Lett. 120 (2018) 063205.
[28] A. Marsman, M. Horbatsch, E.A. Hessels, Deflection of barium monofluoride molecules using the bichromatic force: a density-matrix simulation, Phys. Rev. A 108 (2023) 012811.
[29] Q. Liang, T. Chen, W.-H. Bu, Y.-H. Zhang, B. Yan, Laser cooling with adiabatic passage for type-II transitions, Front. Phys. 16 (2021) 32501.
[30] K. Wenz, I. Kozyryev, R.L. McNally, L. Aldridge, T. Zelevinsky, Large molasses-like cooling forces for molecules using polychromatic optical fields: a theoretical description, Phys. Rev. Res. 2 (2020) 043377.
[31] F. Kogel, M. Rockenhäuser, R. Albrecht, T. Langen, A laser cooling scheme for precision measurements using fermionic barium monofluoride ($^{137}Ba^{19}F$) molecules, New J. Phys. 23 (2021) 095003.
[32] N. Moiseyev, M. Šindelka, L.S. Cederbaum, Trapping of cold atoms in optical lattices by the quadrupole force, Phys. Lett. A 362 (2007) 215–220.
[33] L. Aldridge, S.E. Galica, E.E. Eyler, Simulations of the bichromatic force in multilevel systems, Phys. Rev. A 93 (2016) 013419.
[34] M.A. Chieda, E.E. Eyler, Prospects for rapid deceleration of small molecules by optical bichromatic forces, Phys. Rev. A 84 (2011) 063401.
[35] S.E. Galica, L. Aldridge, E.E. Eyler, Four-color stimulated optical forces for atomic and molecular slowing, Phys. Rev. A 88 (2013) 043418.
[36] X.X. Yang, C.L. Li, Y.N. Yin, S.P. Xu, X.J. Li, Y. Xia, J.P. Yin, Bichromatic slowing of MgF molecules in multilevel systems, J. Phys. B 50 (2017) 015001.
[37] Y.N. Yin, S.P. Xu, M. Xia, Y. Xia, J.P. Yin, Optically stimulated slowing of polar heavy-atom molecules with a constant beat phase, Phys. Rev. A 97 (2018) 043403.
[38] J. Söding, R. Grimm, Y.B. Ovchinnikov, Ph. Bouyer, Ch. Salomon, Short-distance atomic beam deceleration with a stimulated light force, Phys. Rev. Lett. 78 (1997) 1420.
[39] R.X. Gu, K. Yan, D. Wu, J. Wei, Y. Xia, J.P. Yin, radiative force from optical cycling on magnesium monofluoride, Phys. Rev. A 105 (2022) 042806.
[40] M.A. Anderson, M.D. Allen, L.M. Ziurys, Millimeter-wave spectroscopy of MgF: structure and bonding in alkaline-earth monofluoride radicals, J. Chem. Phys. 100 (1994) 824.
[41] S.C. Wright, M. Doppelbauer, S. Hofsäss, H.C. Schewe, B. Sartakov, G. Meijer, S. Truppe, Cryogenic buffer gas beams of AlF, CaF, MgF, YbF, Al, Ca, Yb and NO – a comparison, Mol. Phys. 121 (2022) 17.
[42] M. Xia, R.X. Gu, K. Yan, D. Wu, L. Xu, Y. Xia, J.P. Yin, Destabilization of dark states in MgF molecules, Phys. Rev. A 103 (2021) 013321.
[43] E.S. Shuman, J.F. Barry, D. DeMille, Laser cooling of a diatomic molecule, Nature 467 (2010) 820.
[44] N.R. Hutzler, H.-I. Lu, J.M. Doyle, The Buffer gas Beam: an intense, cold, and slow source for atoms and molecules, Chem. Rev. 112 (2012) 4803.
[45] H.J. Williams, S. Truppe, M. Hambach, L. Caldwell, N.J. Fitch, E.A. Hinds, B. E. Sauer, M.R. Tarbutt, Characteristics of a magneto-optical trap of molecules, New J. Phys. 19 (2017) 113035.
[46] K. Yan, R.X. Gu, D. Wu, J. Wei, Y. Xia, J.P. Yin, Simulation of EOM-based frequency-chirped laser slowing of MgF radicals, Front. Phys. 17 (2022) 42502.
[47] J.J. Hudson, D.M. Kara, I.J. Smallman, B.E. Sauer, M.R. Tarbutt, E.A. Hinds, Improved measurement of the shape of the electron, Nature 473 (2011) 493.
[48] X. Alauze, J. Lim, M.A. Trigatzis, S. Swarbrick, F.J. Collings, N.J. Fitch, B.E. Sauer, M.R. Tarbutt, An ultracold molecular beam for testing fundamental physics, Quantum Sci. Technol. 6 (2021) 044005.
[49] L. Anderegg, N.B. Vilas, C. Hallas, P. Robichaud, A. Jadbabaie, J.M. Doyle, N. R. Hutzler, Quantum control of trapped polyatomic molecules for eEDM searches, Science 382 (2023) 665.
[50] T. Langen, G. Valtolina, D. Wang, J. Ye, Quantum state manipulation and cooling of ultracold molecules, Nat. Phys. 20 (2024) 702.
[51] I.T. Iakubov, A.V. Nedospasov, Cold system of dipolar particles in electric field: bose-Einstein condensation, Phys. Lett. A 232 (1997) 305–307.
[52] N. Bigagli, W. Yuan, S. Zhang, B. Bulatovic, T. Karman, I. Stevenson, S. Will, Observation of Bose–Einstein condensation of dipolar molecules, Nature 631 (2024) 289.